Accepted Manuscript

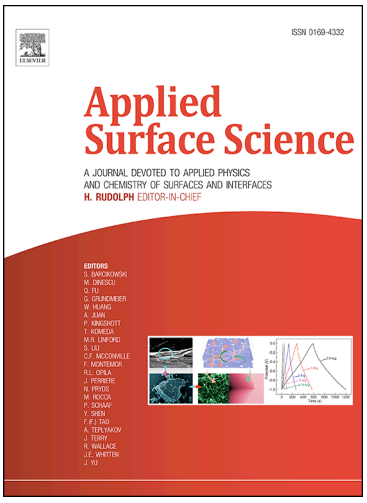

Full Length Article

Effect of Chloride and pH on the Electrochemical Surface Oxidation Enhanced Raman Scattering

Juan V. Perales-Rondon, Sheila Hernandez, Aranzazu Heras, Alvaro Colina

PII: S0169-4332(18)33485-8
DOI: https://doi.org/10.1016/j.apsusc.2018.12.148
Reference: APSUSC 41245

To appear in: *Applied Surface Science*

Received Date: 29 October 2018
Revised Date: 4 December 2018
Accepted Date: 14 December 2018

Please cite this article as: J.V. Perales-Rondon, S. Hernandez, A. Heras, A. Colina, Effect of Chloride and pH on the Electrochemical Surface Oxidation Enhanced Raman Scattering, *Applied Surface Science* (2018), doi: https://doi.org/10.1016/j.apsusc.2018.12.148

This is a PDF file of an unedited manuscript that has been accepted for publication. As a service to our customers we are providing this early version of the manuscript. The manuscript will undergo copyediting, typesetting, and review of the resulting proof before it is published in its final form. Please note that during the production process errors may be discovered which could affect the content, and all legal disclaimers that apply to the journal pertain.

ACCEPTED MANUSCRIPT

Effect of Chloride and pH on the Electrochemical Surface Oxidation Enhanced Raman Scattering

Juan V. Perales-Rondon, Sheila Hernandez, Aranzazu Heras, Alvaro Colina.*

Misael Bañuelos s/n, E-09001 Burgos, Spain

* Corresponding author: acolina@ubu.es

ABSTRACT

In the present work, electrochemical surface oxidation enhanced Raman scattering (EC-SOERS) was studied using time resolved Raman spectroelectrochemistry. This multiresponse technique allows us to obtain dynamic information about the processes taking place during the electrochemical oxidation of a silver substrate. EC-SOERS is particularly found in specific electrolytic conditions, namely, $HClO_4$ 0.1 M + KCl $5 \cdot 10^{-3}$ M, and has a clear dependence on chloride concentration and pH, being the optimum values between $5 \cdot 10^{-3}$ M and $1 \cdot 10^{-2}$ M for chloride and pH = 1. In light of the results of this study, the appearance of the phenomenon is related to the modification of the electrode surface, yielding Ag/AgCl cubes as plasmonic structures, and the stability of such structures at low pH values. The results presented in this work could shed more light into the intricate EC-SOERS phenomenon which can be summarized as the increase of the Raman signal for a Raman probe molecule exclusively during the electrochemical oxidation of silver electrodes.

Keywords: Silver, spectroelectrochemistry, Raman enhancement, nanostructures.

Highlights:

ACCEPTED MANUSCRIPT

- EC-SOERS is particularly present at the electrooxidation of a silver electrode.
- Maximum Raman enhancement was found between 5 and 10 mM of Cl^- and pH=1.
- pH and Cl^- concentration promote and stabilize the Ag/AgCl nanostructures responsible of EC-SOERS.

INTRODUCTION

Recently, a new interesting phenomenon has been published which implies obtaining the enhancement of the Raman signal during the electrochemical oxidation process of a silver electrode [1]. This new phenomenon was denoted as electrochemical surface oxidation enhanced Raman scattering (EC-SOERS). Briefly, when the electrode is roughened in a particular electrolytic media ($HClO_4$/KCl) the appearance of the enhanced Raman signal is exclusively found at anodic potentials. This phenomenon has a clear dependence on both, the modification of the electrode surface and the applied potential. Surface Enhanced Raman Scattering (SERS) [2–6] is a fundamental and general effect that amplifies the Raman signal, mainly by plasmon resonances in the metal substrates, from molecules adsorbed at surface or near the surface. Generally, in EC-SERS the experiment is carried out in a potential window that avoids the oxidation of the substrate [7], in order to preserve the plasmonic structure (at cathodic potentials during an electrochemical roughening procedure). However, for EC-SOERS, the phenomenon takes place at potentials positive enough to ensure the complete surface oxidation of the substrate. The latter raises a new discussion about the mechanism taking place during EC-SOERS. In fact, to the best of our knowledge, EC-SOERS has been reported only one time in literature [1], obtaining a Raman enhanced signal during the electrochemical oxidation of a silver substrate and demonstrating the good performance of the signal for analysis.

In order to obtain a good enhancement in the Raman signal, a proper substrate with plasmonic properties has to be prepared [8,9]. SERS substrates can be prepared in very different ways [2]. Metal roughening procedure is one of the classic methods to do it, in which electrochemistry plays a fundamental role **[10,11]**. Thus, the combination of an electrochemical method with Raman spectroscopy has demonstrated to provide an effective technique to perform a controlled EC-SOERS

ACCEPTED MANUSCRIPT

experiment [1,12]. In this sense, modifying the electrode surface plays a fundamental role in the development of these experiments. In consequence, the study of the modified surface of the silver electrode and how this modification is modulated by different experimental parameters is of capital interest in order to shed more light into the mechanism of the present phenomenon.

In the last years, the use of Raman spectroelectrochemistry (Raman-SEC) has been extended due to the rich information that can be obtained using this technique and because of the significant technical developments [13–18]. Raman-SEC provides information about the vibrational states of molecules, and therefore about their functional groups and structure, concomitantly with its electrochemical activity [19–22]. Additionally, the use of time resolved (TR) experiments provides the control of the applied potential with time (dynamic electrochemistry) [23–25], which makes a difference with the application of discrete potential values (steady state electrochemistry) [12,7]. Thus, TR-SEC allows us to use most of the capabilities of the dynamic electrochemical techniques, opening a wide spectrum of new possibilities such as the characterization of materials in operando conditions, among others [26]. In this sense, the usefulness of TR-Raman-SEC is enhanced when SERS experiments are carried out, because of the much higher sensitivity of the technique that allows us to improve the time resolution. Moreover, using TR-Raman-SEC, the preparation of a SERS substrate by roughening of a plasmonic metal can be achieved by application of a proper potential waveform, and at the same time, the dynamic Raman response can be related to the process taking place at the interface. Because of that, a large number of studies have been devoted to develop new strategies to carry out dynamic Raman-SEC to follow the electrode processes in a rational way [27–29].

Our previous work on EC-SOERS [1] describes this phenomenon and sets a first approach to the experimental conditions to obtain the enhancement during the oxidation of a silver electrode. In the present work, we gain more knowledge about the phenomenon in order to control it in a rational way. With this aim, time resolved Raman spectroelectrochemistry (TR-Raman-SEC) is used to provide valuable *in-situ* information during the electrochemical experiment [30]. Since this

ACCEPTED MANUSCRIPT

phenomenon has been observed under particular electrolytic conditions, a systematic study of different parameters, such as pH and chloride concentration is carried out, in order to shed more light into the role that such experimental conditions have in the modulation of the EC-SOERS response.

MATERIALS AND METHODS

Reagents and solutions

Perchloric acid ($HClO_4$, 60 %, Sigma-Aldrich), uric acid (UA, 99+%, Acros Organics), potassium chloride (KCl, 99+%, Acros Organics) were used. Aqueous solutions were prepared using ultrapure water (18.2 MΩ·cm resistivity at 25 ºC, Milli-Q Direct 8, Millipore).

Instrumentation

Raman spectroelectrochemistry instrument

In situ TR-Raman-SEC was performed by using a SPELEC RAMAN instrument (Metrohm-DropSens), which integrates a laser source of 785 nm. A Raman probe (DRP-RAMANPROBE, Metrohm-DropSens) was connected to the instrument. A home-made cell was used to carry out the experiments using a silver disk electrode. DropView SPELEC software (Metrohm-DropSens) was used to control the instrument, recording real-time and synchronized spectroelectrochemical data.

A home-made silver electrode was used as working electrode. It consists of a silver disk embedded in a cylindrical Teflon tube, allowing an electric contact through a copper wire and silver conductive paint. In this experimental set-up, a home-made Ag/AgCl electrode and a platinum wire were used as reference and counter electrodes, respectively.

Scanning Electron Microscopy

A ZEISS field emission scanning electron microscope (FE-SEM) model Merlin VP Compact was used to characterize the working silver electrodes at various stages of the electrochemical activation. Images were recorded with the secondary electron detector and using an accelerated voltage of 2.0 kV.

ACCEPTED MANUSCRIPT

Raman spectroelectrochemistry measurements

Cyclic voltammetry (CV) was used as electrochemical technique to perform the Raman spectroelectrochemistry experiments. CV was performed between -0.25 V to +0.55 V beginning at +0.10 V in the anodic direction. Unless otherwise stated, a scan rate of 0.02 $V \cdot s^{-1}$ and a step potential of 2 mV were set in all voltammetric experiments. Raman spectra were collected with an integration time of 1 s and a laser power of 80 mW (254 $W \cdot cm^{-2}$). Although 80 mW could be considered high with respect to typical Raman microscopy values found in literature, it should be taken into account that the laser spot size (about 200 μm) is much bigger than the ones used in confocal Raman microscopy, with the energy by surface area being around the typical values or even lower.

Prior to any electrochemical experiment, the electrode was gently polished in a polishing cloth using silica 0.5 μm of particle size. After that, the electrodes were rinsed with abundant ultrapure water, and sonicated for about 2 minutes to eliminate any silica traces.

RESULTS

As was aforementioned, when a silver electrode is roughened under especial electrolytic conditions ($HClO_4$ 0.1 M + KCl $5 \cdot 10^{-3}$ M) with a Raman probe molecule in contact with the electrode during the roughening process, an unexpected and quite interesting behavior is observed. The enhancement of the Raman signal takes place exclusively during the oxidation process provided that a potential is applied to the electrode and was denoted as EC-SOERS [1]. A clear representation of the process is shown in Figure 1, where a SEC experiment is performed using uric acid (UA) as Raman probe, because its molecular structure is suitable to produce EC-SOERS. Figure 1a displays the EC-SOERS spectrum for UA $2 \cdot 10^{-4}$ M + $HClO_4$ 0.1 M + KCl $5 \cdot 10^{-3}$ M at +0.50 V during the TR-Raman-SEC experiment, where the two more important Raman bands for UA (641 cm^{-1} and 1134 cm^{-1}) and Ag-Cl vibration (243 cm^{-1}) can be observed. The EC-SOERS spectrum from 500 to 1700 cm^{-1} belongs unambiguously to UA as was previously demonstrated [1]. It is worth noting that the most intense bands in the EC-SOERS spectrum are related with the deformation or vibration of the ring (641 and 1134 cm^{-1}), unlike those observed in the Raman spectra of solid UA samples [1], of

ACCEPTED MANUSCRIPT

UA solutions (data not shown). Based on this observation, it can be inferred that UA takes a planar conformation during the EC-SOERS experiment on the surface of the substrate. Figure 1b displays a 3D representation of the evolution of the Raman spectrum for UA in these electrolytic conditions, demonstrating the potential of spectroelectrochemistry for obtaining Raman signals with a high time resolution [30]. The analysis of the evolution of the Raman signal with potential (or time) allows us to understand the intrinsic dynamic of a substrate preparation in presence of a Raman probe molecule. Finally, Figure 1c shows the comparison between the linear sweep voltammetry (LSV) for a silver disk electrode (orange curve) with the evolution of the Raman intensity at 641 cm^{-1} for UA during the spectroelectrochemical experiment (blue curve). For simplicity in the terminology used, along this work this representation will be called voltaRamangram at a specific Raman shift. As can be observed, in the anodic direction there is a huge enhancement of the Raman signal. This increase is an unexpected and outstanding behavior for a spectroelectrochemistry experiment and has been explained by the combination of two main effects [1]: (1) the electrochemical surface adsorption of the species (UA) at anodic potentials (due to the electrode polarization), and (2) the interaction of UA with a SERS substrate (Ag^{+}/AgCl or Ag/AgCl complexes) [31–33] formed on the electrode surface at these anodic potentials.

Although sometimes the Raman signal enhancement could be related with an electrochemical reaction of the analyte on the electrode surface, it should be noted that at the applied potentials, there is not electrochemical oxidation of UA, as has been previously demonstrated [1]. Moreover, when the voltammetric experiment is carried out using a gold electrode (under the same experimental conditions), the oxidation of UA takes place at potentials as high as +0.65 V vs Ag/AgCl (data not shown), which is a much higher potential than that used in the EC-SOERS experiments. Furthermore, it can be concluded that no electrochemical UA oxidation is taking place using these experimental conditions

For a better understanding of this interesting process is important to explore how some external parameters, such as pH and chloride concentration, modulate the spectroscopic response.

ACCEPTED MANUSCRIPT

Figure 1

Effect of chloride concentration

It has been stated the importance of the chloride concentration in both, the preparation of a SERS substrate and the modulation of the SERS signal, for a regular SERS experiment [34]. Some authors have discussed about the main role of Cl^- concentration in the formation of active sites in a SERS substrate, particularly for those prepared using a silver electrode [35]. Thus, the so-called "chloride activation" is a key factor for achieving high sensitivity, i.e. single molecule detection (SM-SERS). Here, the effect of chloride concentration in EC-SOERS will be also studied because it plays an essential role in this phenomenon too.

As has been shown above, TR-Raman-SEC provides the evolution of the full spectra during the electrochemical experiment. Thus, a deeper analysis of voltaRamangrams at different Raman shifts can be performed to obtain a whole picture of the electrochemical process. Figure 2 shows the voltaRamangram for UA at 641 cm^{-1} (blue solid curve) and at 243 cm^{-1} (blue dashed curve) obtained in the previous experiment (experimental conditions in Fig 1. and experimental section). The band around 641 cm^{-1} is one of the most characteristic Raman bands for UA related to the skeletal ring deformation [36,37], whereas the signal at 243 cm^{-1} is related to the Ag-Cl bond vibration, widely reported in the literature.[34,35,38] Moreover, time resolved measurements allow us to obtain the derivative with time of the voltaRamangram at 243 cm^{-1} (orange solid curve in Fig. 2). When the two voltaRamangrams are compared, a clear relationship between them along the spectroelectrochemistry experiment can be found. At +0.20 V both signals start to increase, being the Ag-Cl band the one that shows the highest increase until reaching a maximum around +0.40 V, moment at which the UA signal increases sharply. Above +0.40 V, the Ag-Cl signal falls down concomitantly with the increase of the UA signal up to +0.50 V, where the UA band reaches a maximum.

The analysis of the derivative voltaRamangram at 243 cm^{-1} with time reveals two clear regions (Fig. 2, orange curve). The first one, between +0.20 V and +0.30 V, where the rate of increase of the

ACCEPTED MANUSCRIPT

Ag-Cl band rises during the initial generation of AgCl particles [1,30,34,38] on the electrode surface. And the second one, peaking around +0.45 V, when the derivative signal sharply decreases during the highest increase for UA band at 641 cm^{-1}. The fact that, when the UA band grows (641 cm^{-1}) the Ag-Cl signal decreases (243 cm^{-1}), is directly related with the adsorption properties of the two compounds, UA and Cl^-. Thus, it is clear that above +0.20 V chloride adsorption is highly favored by the electrode polarization, however, when the potential increases, UA begins to adsorb on the nanostructured electrode surface, replacing Cl^- species and producing an enhancement in the Raman signal. For this reason, the Ag-Cl band dramatically decreases at higher potentials. This result indicates that there is a clear relationship between the generation of the Ag-Cl species and the enhancement of the Raman signal of UA.

An important issue on the increase of the Raman signal is the presence of charge transfer phenomena [39–41], which is the main contribution to the chemical mechanism in the SERS effect. A deeper analysis of the evolution of the Ag-Cl Raman band with potential has revealed almost no change in the Raman shift, compared with the typical changes observed in the cathodic direction for an EC-SERS experiment. In EC-SOERS, Raman signal at 243 cm^{-1} is related to the generation of AgCl salt nanostructures during the oxidation process. Charge transfer and surface coverage (dipole-dipole interaction) of adsorbed chloride ions is observed only in the cathodic scan (data not shown), where silver is deposited on the electrode surface with the Raman intensity and Raman band shifting following the same trend. This is another difference between EC-SOERS and EC-SERS.

Figure 2

Once described the clear relationship between the Ag-Cl and the UA bands, a systematic study using different Cl^- concentration was performed. Figure 3 shows the voltaRamangrams at different Cl^- concentrations, for UA at 641 cm^{-1} and, in order to establish the influence of Cl^-, at 243 cm^{-1}.

As can be observed, when the silver electrode is oxidized, the maximum Raman intensity at 641 cm^{-1}, related to the UA, clearly depends on the chloride concentration. This Raman signal at 641 cm^{-1} reaches a maximum value between 5 mM and 10 mM of Cl^-, as is shown in Table 1. In fact, when

ACCEPTED MANUSCRIPT

using both, a too low or a too high chloride concentration, uric acid signal during the electrochemical oxidation of silver vanishes. On the other hand, orange curves and results in Table 1 show the decreasing onset potential when the UA Raman signal is observed. Again, the minimum is located between 5 mM and 10 mM of Cl^-. These results suggest the existence of an optimum Cl^- concentration in order to promote the EC-SOERS effect. Additionally, the electrical charge associated with the first silver oxidation peak decreases as the Cl^- concentration diminishes (see orange curves in Figure 3). As was stated in our previous work, this peak is directly associated with the AgCl formation on the electrode surface [1]. Thus, the controlled formation of AgCl is mandatory to promote the increase of Raman signal at anodic potentials.

Moreover, Figure 3 also shows that the Raman signal at 243 cm^{-1} has a similar behavior with the band associated with UA, but shifted in potential. Chloride band starts to increase at potentials lower than UA band, as was stated before, but the maximum Raman enhancement is also found between 5 mM and 10 mM. It is noteworthy that 243 cm^{-1} band is only correlated with the chloride concentration until 10 mM, decreasing the Raman intensity after this concentration, with a behavior of the voltaRamangram quite different not only to that observed for other chloride concentration but also for UA. At the highest concentrations of chloride, the onset potential is shifted to less positive potentials, and there are two maxima in the voltaRamangrams, one emerges at the early oxidation stage and the other one at potentials around +0.40 V. Additionally, the maximum for the voltaRamangram at 243 cm^{-1} seems to achieve a plateau for the evolution of the Ag-Cl band. From these results, it can be concluded that at very high chloride concentrations there is not UA adsorption on the silver substrate because UA cannot replace Cl^- species on the AgCl particles, and at very low concentrations there are few AgCl particles and the effect of adsorption of UA is not high enough to be significant.

Table 1

ACCEPTED MANUSCRIPT

Figure 3

Effect of pH

Figure 4 displays the voltaRamangrams at 641 cm^{-1} for UA in the general media UA $2 \cdot 10^{-4}$ M + $HClO_4$ X M + $KClO_4$ (0.1-X) M + KCl $5 \cdot 10^{-3}$ M at three different pH values, compared to the evolution of the voltaRamangrams at 243 cm^{-1} obtained in the same experiments. As has been stated above, Raman band at 641 cm^{-1} is characteristic of UA, whereas the signal related to Ag-Cl is found at 243 cm^{-1} [35,42].

Figure 4

Table 2

As can be observed in Figure 4 and Table 2, the Raman signal in the voltaRamangram at 641 cm^{-1} decreases and the onset potential diminishes as pH increases. Furthermore, as has been observed in the study of the effect of Cl^- concentration, the maximum of the voltaRamangram at 243 cm^{-1} coincides with the beginning of the EC-SOERS signal, which suggests a clear interaction between the formation of Ag-Cl and the observation of EC-SOERS signal for UA in these conditions. It is worth noting that, despite Cl^- concentration remains constant under these experiments and only the pH of the solution changes, there is still a variation in the shape of the voltaRamangram for the Ag-Cl signal. In fact, the higher the pH, the lower the maximum value for the Raman signal at 243 cm^{-1}. The result for the highest pH studied is quite similar to the effect of Cl^- concentration higher than 50 mM in Figure 3. This fact is particularly interesting because implies that, at high pH values, the generation of Ag-Cl competes with the formation of silver oxides, as is suggested by the evolution of a band around 430 cm^{-1} related to the generation of silver oxide (results not shown).[43,44] Therefore, the process that yields an enhancement of the Raman intensity at anodic potentials is favored at low pH values. That is to say, the species responsible for the Raman enhancement are less stable or are not formed at high pH values, being the optimum conditions an electrolytic medium 0.1

ACCEPTED MANUSCRIPT

M $HClO_4$. It should be noted that solutions with a pH more acidic than 1 did not yield good results with a very poor enhancement of the UA Raman signal.

Scanning electron microscopy analysis

As has been demonstrated above, Raman enhancement during the electrochemical oxidation of silver is a process that highly depends on the chloride concentration. In order to understand this complex surface process is necessary to explore the role of the chloride concentration in the modification of the substrate during the spectroelectrochemistry experiment. For this reason, an *ex-situ* SEM study is helpful to shed more light on the origin of the EC-SOERS signal. Samples were obtained after performing a linear sweep voltammetry on a silver disk electrode with a solution containing UA $2 \cdot 10^{-4}$ M + $HClO_4$ 0.1 M + KCl X M. The potential was stopped at +0.55 V for each chloride concentration. Once stopped the electrochemical experiment, the electrode was rinsed with ultrapure water and stored in a dark and dry environment to avoid or minimize the changes on the electrode surface until obtaining the SEM images.

Figure 5 shows the SEM images for 6 different electrodes oxidized under similar electrochemical conditions, but changing the chloride concentration from 0.5·mM to 100 mM.

As can be inferred from Figure 5, the higher the chloride concentration, the higher amount of AgCl particles is formed. Thus, while in Figure 5A, at the lowest Cl^- concentration, the surface remains almost unchanged, in Figure 5F, at the highest Cl^- concentration, the surface is completely covered by AgCl. Additionally, as the chloride concentration is increased, AgCl particles grow in size and their shape changes, becoming amorphous at high Cl^- concentrations. As was stated above, the higher enhancement of the Raman signal is found between $5 \cdot 10^{-3}$ M and $1 \cdot 10^{-2}$ M of KCl. The corresponding images (Fig. 5C and 5D, respectively) have a feature in common, which is the discrete formation of cubic AgCl particles that are not extended over the whole surface but are interconnected between them, forming chains of cubic particles. A detailed examination of these images (zoom images in Figure 5) reveals that some small nanoparticles are deposited upon the

ACCEPTED MANUSCRIPT

cubic AgCl particles. All these features seem to play a key role in the formation of high performance plasmonic structures [45,46].

Figure 5

As was described in the previous section, EC-SOERS was also studied at different pH. Figure 6 shows the corresponding SEM images for three different silver electrodes during the electrochemical oxidation at +0.55 V in UA $2 \cdot 10^{-4}$ M + $HClO_4$ X M + $KClO_4$ (0.1-X) M + KCl $5 \cdot 10^{-3}$ M at three different pHs, namely, 1, 2 and 3.4.

As can be observed, the three images are quite similar in morphology, with the particular difference that the amount of AgCl particles decreases with the increase of pH. Additionally, as the pH increases the interconnection between these particles is lost and a more homogeneous distribution of the AgCl particles is observed. In this case, the formation of small nanoparticles on the facets of the AgCl cubes is quite similar for all the studied pH.

Figure 6

DISCUSSION

As was shown in a previous work [1], the presence of special electrolytic conditions ($HClO_4$/KCl) is critical to obtain a Raman enhancement during the electrochemical oxidation stage of silver electrodes. In view of the new set of experiments shown in this work, a more detailed description of EC-SOERS and new interpretations about this process can be drawn as follows.

There are two key factors for the appearance of EC-SOERS on a silver electrode. One of them lies in the chloride concentration and the other resides in the pH of the solution. Both of them are related to the formation of well-defined AgCl cubes. In order to obtain a clear EC-SOERS behavior, chloride concentration has to be found between $5 \cdot 10^{-3}$ M and $1 \cdot 10^{-2}$ M. These particular values seem to be ideal for the formation of AgCl cubic particles interconnected with each other. From SEM analysis of these substrates, we can affirm that the formation of AgCl cubic particles itself is not the unique key factor for the enhancement of the Raman signal at the oxidation stage. The interconnection between them seems to be crucial. So far, AgCl has not been reported as a

ACCEPTED MANUSCRIPT

plasmonic substrate, but some recent works have explored the properties of Ag/AgCl material, arguing some plasmonic properties.[31–33] In fact, those studies have demonstrated the usefulness of those structures as photocatalysts and antibacterial substances [32,47,48]. Additionally, other authors have reported the enhancement of the Raman signal using Ag/AgCl as a substrate by a pretreatment of cubic AgCl particles with a radiation source [48]. All previous works have concluded that placing some Ag particles or Ag^+ on the surface of the AgCl cubes is mandatory for obtaining a reasonable Raman signal enhancement. According with these published works and with our results, we propose that the electrochemical oxidation plays the role of modifying the AgCl cubes by placing Ag^+ or Ag particles on the surface. Additionally, the role of the adsorption of the target molecule on the Ag/AgCl structures is also fundamental to obtain a good EC-SOERS response. As has been shown in Fig. 2, when the target molecule is adsorbed on the nanostructured surface, chloride is replaced producing an enhancement in the Raman signal.

In view of the results shown above, the formation of such specific Ag/AgCl structures is clear in the experiments that shown an EC-SOERS signal. Moreover, these structures were only obtained in an optimum range of chloride concentration. Thus, at high chloride concentrations, AgCl cubes became amorphous, and at a lower chloride concentration, AgCl cubes were not formed. In these two limiting cases, EC-SOERS was not observed. This chloride concentration range can be easily explained by the mass transport found under these experimental conditions. Thus, as chloride is quite diluted on the electrode surface, its rate of compensation by a diffusion control is low compared to the rate of consumption. This allows the AgCl, once formed as a seed, growth slowly until obtaining an ordered cube like structure.

The second key factor for obtaining an EC-SOERS signal is definitively the acidity of the solution. As has been demonstrated above, the higher Raman enhancement is obtained for acidic solutions, with pH 1 being the best one to carry out EC-SOERS experiments. Again, the reason for such observation lies in providing a suitable environment for the formation of Ag/AgCl cubes because silver oxide can be easily generated by increasing the pH. Thus, formation of AgCl at less

ACCEPTED MANUSCRIPT

acidic solution is somehow inhibited. In fact, Figure 6 has demonstrated that at the highest pH selected, the formation of AgCl structure is less favored, being formed less and smaller AgCl cubes. Moreover, at that pH, a band related to the generation of silver oxide [43,44] around 430 cm^{-1} is observed. Therefore, the lower amount of interconnected Ag/AgCl cubes, the lower EC-SOERS signal is obtained, as is shown in Figure 4.

Finally, all these observations indicate not only the complexity of the EC-SOERS phenomenon, but also the possibilities of obtaining new plasmonic surfaces by modulating the electrolytic conditions during a spectroelectrochemical experiment.

CONCLUSIONS

The results presented in this work shed more light on the complex EC-SOERS phenomenon which can be summarized as the increase of the Raman signal during the electrochemical oxidation of the silver electrode surface. This phenomenon is particularly evident under specific electrolytic conditions, with the enhancement being optimum for a chloride concentration between $5 \cdot 10^{-3}$ M and $1 \cdot 10^{-2}$ M and pH=1. Both conditions directly favor the formation of Ag/AgCl cubic structures on the electrode surface. Adsorption/desorption of chloride observed during the experiments confirm that the target molecule is highly adsorbed on the Ag/AgCl structures when the Raman signal is enhanced.

Once described the particular conditions to obtain this phenomenon, more work should be done for a better characterization of the nanostructures using more powerful *in-situ* techniques. Undoubtedly, the search for new nanostructures that provide EC-SOERS should be fundamental to find out whether we are facing a universal phenomenon.

ACKNOWLEDGMENTS

Authors acknowledge the financial support from Ministerio de Economía y Competitividad (Grants CTQ2017-83935-R-AEI/FEDERUE) and Junta de Castilla y León (Grant BU033-U16). J.V.P-R. thanks JCyL for his postdoctoral fellowship (Grant BU033-U16). S.H. thanks its contract

ACCEPTED MANUSCRIPT

funded by JCyL, the European Social Fund and the Youth Employment Initiative. Authors thank Jesus Garoz-Ruiz for critical reading of the manuscript and helpful discussion.

AUTHOR INFORMATION

Corresponding Author

*E-mail: acolina@ubu.es

Notes

The authors declare no competing financial interest.

REFERENCES

[1] J. V. Perales-Rondon, S. Hernandez, D. Martin-Yerga, P. Fanjul-Bolado, A. Heras, A. Colina, Electrochemical surface oxidation enhanced Raman scattering, Electrochim. Acta. 282 (2018) 377–383. doi:10.1016/j.electacta.2018.06.079.

[2] B. Sharma, R.R. Frontiera, A.-I. Henry, E. Ringe, R.P. Van Duyne, SERS: Materials, applications, and the future, Mater. Today. 15 (2012) 16–25. doi:10.1016/S1369-7021(12)70017-2.

[3] S. Schlücker, Surface-Enhanced Raman Spectroscopy: Concepts and Chemical Applications, Angew. Chemie Int. Ed. 53 (2014) 4756–4795. doi:10.1002/anie.201205748.

[4] J. Kneipp, H. Kneipp, K. Kneipp, SERS—a single-molecule and nanoscale tool for bioanalytics, Chem. Soc. Rev. 37 (2008) 1052–1060. doi:10.1039/b708459p.

[5] A. Otto, Surface enhanced Raman scattering (SERS), what do we know?, Appl. Surf. Sci. 6 (1980) 309–355. doi:10.1016/0378-5963(80)90020-3.

[6] C. Muehlethaler, M. Leona, J.R. Lombardi, Review of Surface Enhanced Raman Scattering Applications in Forensic Science, Anal. Chem. 88 (2016) 152–169. doi:10.1021/acs.analchem.5b04131.

ACCEPTED MANUSCRIPT

[7] D.-Y. Wu, J.-F. Li, B. Ren, Z.-Q. Tian, Electrochemical surface-enhanced Raman spectroscopy of nanostructures, Chem. Soc. Rev. 37 (2008) 1025–1041. doi:10.1039/b707872m.

[8] A. Manshina, A. Povolotskiy, A. Povolotckaia, A. Kireev, Y. Petrov, S. Tunik, Annealing effect: Controlled modification of the structure, composition and plasmon resonance of hybrid Au–Ag/C nanostructures, Appl. Surf. Sci. 353 (2015) 11–16. doi:10.1016/j.apsusc.2015.06.048.

[9] M. Pisarek, R. Nowakowski, A. Kudelski, M. Holdynski, A. Roguska, M. Janik-Czachor, E. Kurowska-Tabor, G.D. Sulka, Surface modification of nanoporous alumina layers by deposition of Ag nanoparticles. Effect of alumina pore diameter on the morphology of silver deposit and its influence on SERS activity, Appl. Surf. Sci. 357 (2015) 1736–1742. doi:10.1016/j.apsusc.2015.10.011.

[10] Z.-Q. Tian, B. Ren, D.-Y. Wu, Surface-Enhanced Raman Scattering: From Noble to Transition Metals and from Rough Surfaces to Ordered Nanostructures, J. Phys. Chem. B. 106 (2002) 9463–9483. doi:10.1021/jp0257449.

[11] X.-M.M. Lin, Y. Cui, Y.-H.H. Xu, B. Ren, Z.-Q.Q. Tian, Surface-enhanced Raman spectroscopy: substrate-related issues., Anal. Bioanal. Chem. 394 (2009) 1729–45. doi:10.1007/s00216-009-2761-5.

[12] Z. Tian, X. Zhang, Developments in Electrochemistry, John Wiley & Sons, Ltd, Chichester, UK, 2014. doi:10.1002/9781118694404.

[13] C. Zong, C.-J. Chen, M. Zhang, D.-Y. Wu, B. Ren, Transient Electrochemical Surface-Enhanced Raman Spectroscopy: A Millisecond Time-Resolved Study of an Electrochemical Redox Process, J. Am. Chem. Soc. 137 (2015) 11768–11774. doi:10.1021/jacs.5b07197.

[14] Y. Zhai, Z. Zhu, S. Zhou, C. Zhu, S. Dong, Recent advances in spectroelectrochemistry,

ACCEPTED MANUSCRIPT

Nanoscale. 10 (2018) 3089–3111. doi:10.1039/c7nr07803j.

[15] A.J. Wilson, N.Y. Molina, K.A. Willets, Modification of the Electrochemical Properties of Nile Blue through Covalent Attachment to Gold As Revealed by Electrochemistry and SERS, J. Phys. Chem. C. 120 (2016) 21091–21098. doi:10.1021/acs.jpcc.6b03962.

[16] M. Kalbac, H. Farhat, J. Kong, P. Janda, L. Kavan, M.S. Dresselhaus, Raman Spectroscopy and in Situ Raman Spectroelectrochemistry of Bilayer 12 C/ 13 C Graphene, Nano Lett. 11 (2011) 1957–1963. doi:10.1021/nl2001956.

[17] B. Bozzini, L. D'Urzo, C. Mele, V. Romanello, A SERS Investigation of Cyanide Adsorption and Reactivity during the Electrodeposition of Gold, Silver, and Copper from Aqueous Cyanocomplexes Solutions, J. Phys. Chem. C. 112 (2008) 6352–6358. doi:10.1021/jp0726539.

[18] L. León, J.D. Mozo, Designing spectroelectrochemical cells: A review, TrAC Trends Anal. Chem. 102 (2018) 147–169. doi:10.1016/j.trac.2018.02.002.

[19] G. Niaura, A.K. Gaigalas, V.L. Vilker, Moving spectroelectrochemical cell for surface Raman spectroscopy, J. Raman Spectrosc. 28 (1997) 1009–1011. doi:10.1002/(SICI)1097-4555(199712)28:12<1009::AID-JRS196>3.0.CO;2-G.

[20] F.J. Vidal-Iglesias, J. Solla-Gullón, J.M. Orts, A. Rodes, J.M. Pérez, J.M. Feliu, SERS on (111) Surface Nanofacets at Pt Nanoparticles: The Case of Acetaldehyde Oxime Reduction, J. Phys. Chem. C. 116 (2012) 10781–10789. doi:10.1021/jp300748f.

[21] R. Mažeikienė, A. Statino, Z. Kuodis, G. Niaura, A. Malinauskas, In situ Raman spectroelectrochemical study of self-doped polyaniline degradation kinetics, Electrochem. Commun. 8 (2006) 1082–1086. doi:10.1016/j.elecom.2006.04.017.

[22] R. Mažeikienė, G. Niaura, O. Eicher-Lorka, A. Malinauskas, Raman spectroelectrochemical

ACCEPTED MANUSCRIPT

study of Meldola blue, adsorbed and electropolymerized at a gold electrode, J. Colloid Interface Sci. 357 (2011) 189–197. doi:10.1016/j.jcis.2011.01.086.

[23] L. Dunsch, Recent Advances in in situ multi-spectroelectrochemistry, J. Solid State Electrochem. 15 (2011) 1631–1646. doi:10.1007/s10008-011-1453-1.

[24] C. Shi, W. Zhang, R.L. Birke, J.R. Lombardi, Detection of short-lived intermediates in electrochemical reactions using time-resolved surface-enhanced Raman spectroscopy, J. Phys. Chem. 94 (1990) 4766–4769. doi:10.1021/j100375a004.

[25] M. Wang, T. Spataru, J.R. Lombardi, R.L. Birke, Time Resolved Surface Enhanced Raman Scattering Studies of 3-Hydroxyflavone on a Ag Electrode, J. Phys. Chem. C. 111 (2007) 3044–3052. doi:10.1021/jp0650937.

[26] Y. Deng, L.R.L. Ting, P.H.L. Neo, Y.-J. Zhang, A.A. Peterson, B.S. Yeo, Operando Raman Spectroscopy of Amorphous Molybdenum Sulfide (MoS x) during the Electrochemical Hydrogen Evolution Reaction: Identification of Sulfur Atoms as Catalytically Active Sites for H + Reduction, ACS Catal. 6 (2016) 7790–7798. doi:10.1021/acscatal.6b01848.

[27] Z.-Q. Tian, B. Ren, Adsorption and Reaction at Electrochemical Interfaces as Probed by Surface-Enhanced Raman Spectroscopy, Annu. Rev. Phys. Chem. 55 (2004) 197–229. doi:10.1146/annurev.physchem.54.011002.103833.

[28] S. Park, P. Yang, P. Corredor, M.J. Weaver, Transition Metal-Coated Nanoparticle Films: Vibrational Characterization with Surface-Enhanced Raman Scattering, J. Am. Chem. Soc. 124 (2002) 2428–2429. doi:10.1021/ja017406b.

[29] S. Zou, M.J. Weaver, Surface-Enhanced Raman Scattering on Uniform Transition-Metal Films: Toward a Versatile Adsorbate Vibrational Strategy for Solid-Nonvacuum Interfaces?, Anal. Chem. 70 (1998) 2387–2395. doi:10.1021/ac9800154.

ACCEPTED MANUSCRIPT

[30] D. Martín-Yerga, A. Pérez-Junquera, M.B. González-García, J. V. Perales-Rondon, A. Heras, A. Colina, D. Hernández-Santos, P. Fanjul-Bolado, Quantitative Raman spectroelectrochemistry using silver screen-printed electrodes, Electrochim. Acta. 264 (2018) 183–190. doi:10.1016/j.electacta.2018.01.060.

[31] Z. Gan, A. Zhao, M. Zhang, D. Wang, W. Tao, H. Guo, D. Li, M. Li, Q. Gao, A facile strategy for obtaining fresh Ag as SERS active substrates, J. Colloid Interface Sci. 366 (2012) 23–27. doi:10.1016/J.JCIS.2011.09.052.

[32] N. Zhao, X. Fei, X. Cheng, J. Yang, Synthesis of silver/silver chloride/graphene oxide composite and its surface-enhanced Raman scattering activity and self-cleaning property, IOP Conf. Ser. Mater. Sci. Eng. 242 (2017) 12002. doi:10.1088/1757-899X/242/1/012002.

[33] L. Dawn, W. Jian, X. Houwen, S. Xu, L. Fan-chen, Enhancement origin of SERS from pyridine adsorbed on AgCl colloids, Spectrochim. Acta Part A Mol. Spectrosc. 43 (1987) 379–382. doi:10.1016/0584-8539(87)80120-4.

[34] Y.S. Li, J. Cheng, Y. Wang, Surface-enhanced Raman spectra of dyes and organic acids in silver solutions: Chloride ion effect, Spectrochim. Acta - Part A Mol. Biomol. Spectrosc. 56 (2000) 2067–2072. doi:10.1016/S1386-1425(00)00268-7.

[35] A. Otto, A. Bruckbauer, Y.. Chen, On the chloride activation in SERS and single molecule SERS, J. Mol. Struct. 661–662 (2003) 501–514. doi:10.1016/j.molstruc.2003.07.026.

[36] L. Zhao, J. Blackburn, C.L. Brosseau, Quantitative Detection of Uric Acid by Electrochemical-Surface Enhanced Raman Spectroscopy Using a Multilayered Au/Ag Substrate, Anal. Chem. 87 (2015) 441–447. doi:10.1021/ac503967s.

[37] C. Westley, Y. Xu, B. Thilaganathan, A.J. Carnell, N.J. Turner, R. Goodacre, Absolute Quantification of Uric Acid in Human Urine Using Surface Enhanced Raman Scattering with the Standard Addition Method, Anal. Chem. 89 (2017) 2472–2477.

ACCEPTED MANUSCRIPT

doi:10.1021/acs.analchem.6b04588.

[38] R. Pang, X.-G. Zhang, J.-Z. Zhou, D.-Y. Wu, Z.-Q. Tian, SERS Chemical Enhancement of Water Molecules from Halide Ion Coadsorption and Photoinduced Charge Transfer on Silver Electrodes, J. Phys. Chem. C. 121 (2017) 10445–10454. doi:10.1021/acs.jpcc.7b02408.

[39] P. Kambhampati, C.M. Child, M.C. Foster, A. Campion, On the chemical mechanism of surface enhanced Raman scattering: Experiment and theory, J. Chem. Phys. 108 (1998) 5013–5026. doi:10.1063/1.475909.

[40] A. Otto, I. Mrozek, H. Grabhorn, W. Akemann, Surface-enhanced Raman scattering, J. Phys. Condens. Matter. 4 (1992) 1143–1212. doi:10.1088/0953-8984/4/5/001.

[41] L. Jensen, C.M. Aikens, G.C. Schatz, Electronic structure methods for studying surface-enhanced Raman scattering, Chem. Soc. Rev. 37 (2008) 1061–1073. doi:10.1039/b706023h.

[42] D.D. Tuschel, J.E. Pemberton, J.E. Cook, SERS and SEM of roughened silver electrode surfaces formed by controlled oxidation-reduction in aqueous chloride media, Langmuir. 2 (1986) 380–388. doi:10.1021/la00070a002.

[43] R. Kötz, E. Yeager, Raman studies of the silver/silver oxide electrode, J. Electroanal. Chem. Interfacial Electrochem. 111 (1980) 105–110. doi:10.1016/S0022-0728(80)80080-5.

[44] J. Deng, X. Xu, J. Wang, Y. Liao, B. Hong, In situ surface Raman spectroscopy studies of oxygen adsorbed on electrolytic silver, Catal. Letters. 32 (1995) 159–170. doi:10.1007/BF00806111.

[45] Y. Kang, K.J. Erickson, T.A. Taton, Plasmonic nanoparticle chains via a morphological, sphere-to-string transition, J. Am. Chem. Soc. 127 (2005) 13800–13801. doi:10.1021/ja055090s.

[46] N. Harris, M.D. Arnold, M.G. Blaber, M.J. Ford, Plasmonic Resonances of Closely Coupled

ACCEPTED MANUSCRIPT

Gold Nanosphere Chains, J. Phys. Chem. C. 113 (2009) 2784–2791. doi:10.1021/jp8083869.

[47] Z.Y. Lin, J. Xiao, J.H. Yan, P. Liu, L.H. Li, G.W. Yang, Ag/AgCl plasmonic cubes with ultrahigh activity as advanced visible-light photocatalysts for photodegrading dyes, J. Mater. Chem. A. 3 (2015) 7649–7658. doi:10.1039/c5ta00942a.

[48] C. Dong, Z. Yan, J. Kokx, D.B. Chrisey, C.Z. Dinu, Antibacterial and surface-enhanced Raman scattering (SERS) activities of AgCl cubes synthesized by pulsed laser ablation in liquid, Appl. Surf. Sci. 258 (2012) 9218–9222. doi:10.1016/j.apsusc.2011.07.076.

ACCEPTED MANUSCRIPT

ACCEPTED MANUSCRIPT

Figure captions:

Figure 1. (A) EC-SOERS spectrum for UA at +0.50 V during a spectroelectrochemical experiment. Spectra shown from 100 to 1800 cm^{-1}. (B) 3D surface that represents the evolution of EC-SOERS spectra for UA during the TR-Raman-SEC experiment on a silver disk electrode between +0.125 V to +0.55 V in the anodic direction. (C) Comparison between the voltammetric signal (orange curve) for a silver disk electrode and the voltaRamangram for UA at 641 cm^{-1} (blue curve). Raman spectra were collected during the voltammetric experiment using an integration time of 1 s. Laser: 785 nm with a power of 80 mW (254 $W \cdot cm^{-2}$). LSV from +0.125 V to +0.55 V. Scan rate: 0.02 $V \cdot s^{-1}$. Working solution: UA $2 \cdot 10^{-4}$ M + $HClO_4$ 0.1 M + KCl $5 \cdot 10^{-3}$ M.

Figure 2. VoltaRamangrams at 641 cm^{-1} (blue solid curve) and 243 cm^{-1} (blue dashed curve) compared to the derivative of the voltaRamangram with time at 243 cm^{-1} (orange solid curve) for a spectroelectrochemistry experiment of UA $2 \cdot 10^{-4}$ M + $HClO_4$ 0.1 M + KCl $5 \cdot 10^{-3}$ M. The LSV was carried out from +0.125 V to +0.55 V in the anodic direction on a silver disk electrode (Fig. 1C, orange curve). Scan rate: 0.02 $V \cdot s^{-1}$. Raman spectra were taken at 1 s of integration time with a 785 nm laser.

Figure 3. VoltaRamangrams at 641 cm^{-1} (red curve) and at 243 cm^{-1} (blue curve), and linear sweep voltammetry (orange curve) for the spectroelectrochemistry experiments with a silver disk electrode in UA $2 \cdot 10^{-4}$ M + $HClO_4$ 0.1 M + KCl X M (different Cl^- concentrations). From left to right are represented the chloride concentration in increasing order, from 0.05 mM to 100 mM. Spectroelectrochemistry experimental conditions are the same as in Figure 1.

Figure 4. VoltaRamangrams at 641 cm^{-1} (red curve) and at 243 cm^{-1} (blue curve) for a spectroelectrochemistry experiment of a silver disk electrode in UA $2 \cdot 10^{-4}$ M + $HClO_4$ X M + $KClO_4$ (0.1-X) M + KCl 5.10^{-3} M at three different pH values. Spectroelectrochemistry experimental conditions are the same as in Figure 1.

ACCEPTED MANUSCRIPT

Figure 5. SEM images for a silver disk electrode during an oxidation process in UA $2 \cdot 10^{-4}$ M + $HClO_4$ 0.1 M + KCl X M for different concentrations of KCl. KCl concentration: (A) 0.5 mM; (B) 1 mM; (C) 5 mM; (D) 10 mM; (E) 50 mM; (F) 100 mM. Images were taken at 5000X and 25000X (insets).

Figure 6. SEM images for a silver disk electrode during an oxidation process in UA $2 \cdot 10^{-4}$ M + $HClO_4$ X M + $KClO_4$ (0.1-X) M + KCl $5 \cdot 10^{-3}$ M at different pH. (A) pH=1; (B) pH=2; (C) pH=3.4. Images were taken at 5000X and 25000X (insets).

ACCEPTED MANUSCRIPT

Figures

Figure 1.

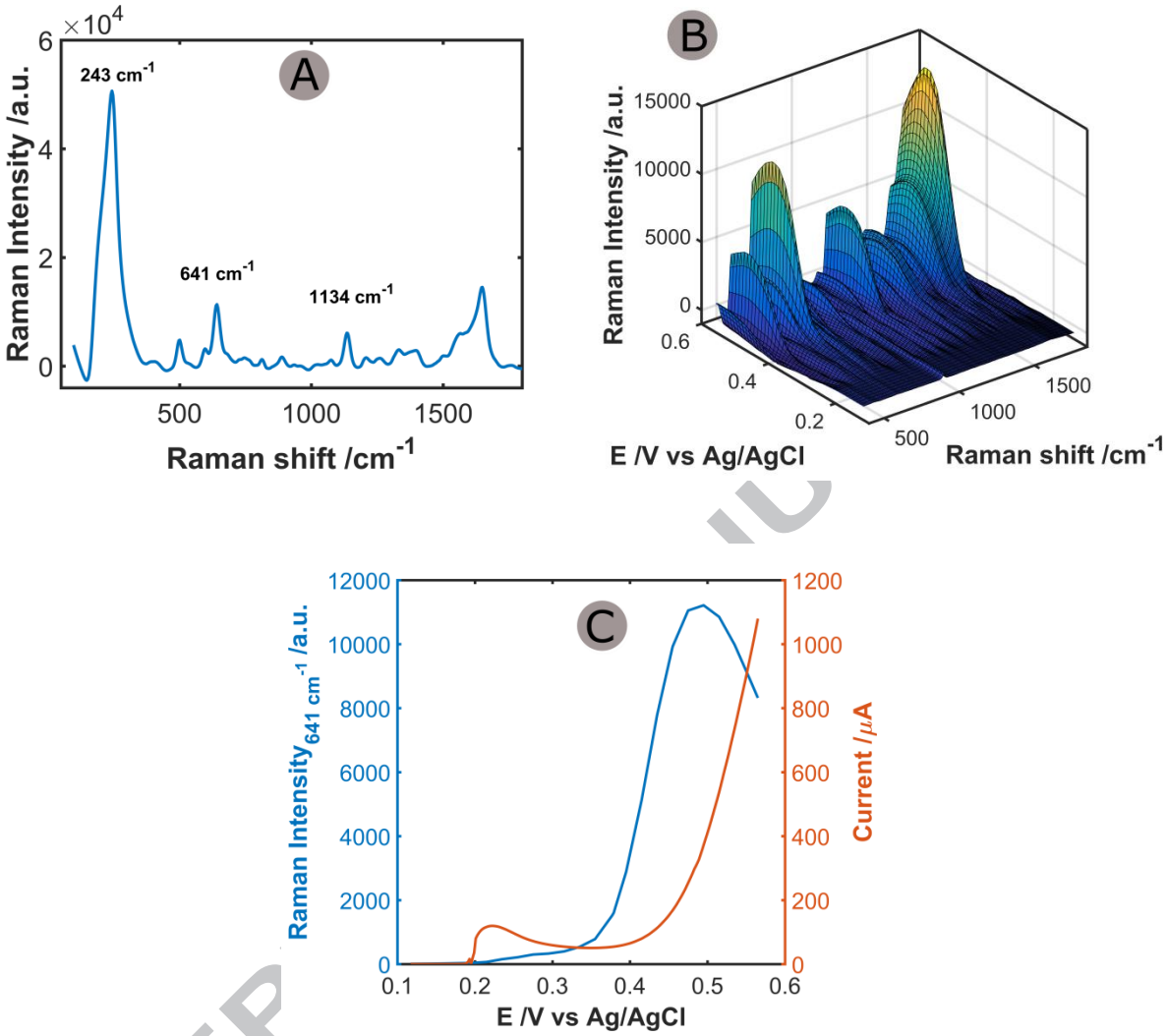

ACCEPTED MANUSCRIPT

ACCEPTED MANUSCRIPT

Figure 2.

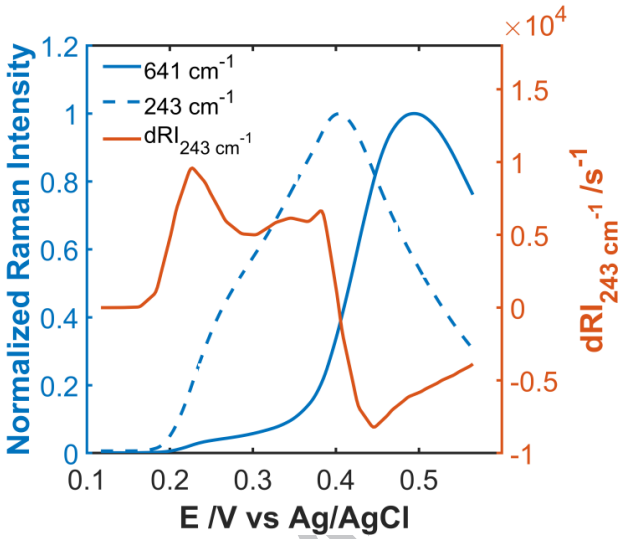

ACCEPTED MANUSCRIPT

Figure 3.

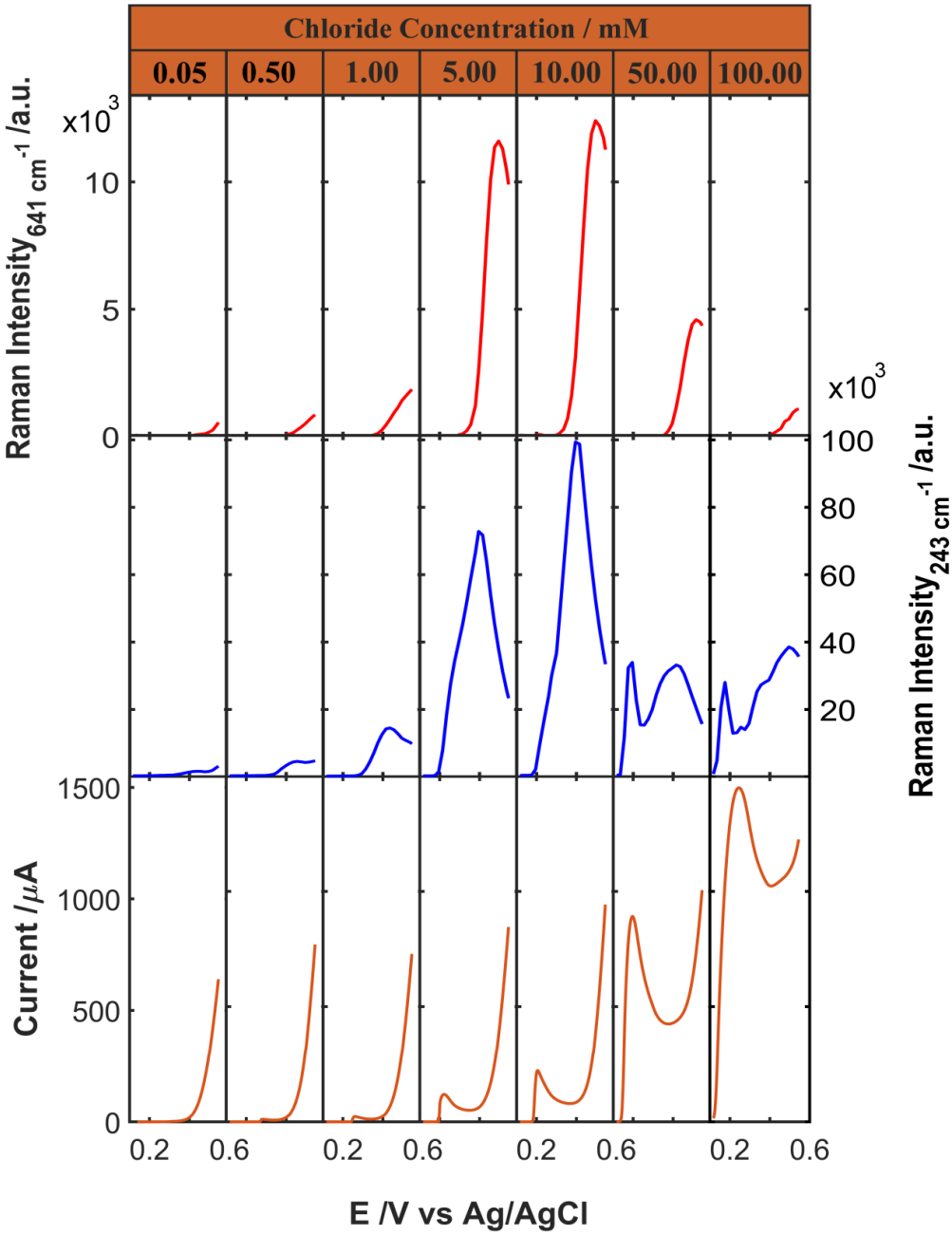
Chloride Concentration / mM
0.05
0.50
1.00
5.00
10.00
50.00
100.00
Raman Intensity641 cm-1 /a.u.
x10^3
10
5
0
Raman Intensity243 cm-1 /a.u.
x10^3
100
80
60
40
20
Current /μA
1500
1000
500
0
0.2
0.6
E /V vs Ag/AgCl

ACCEPTED MANUSCRIPT

Figure 4.

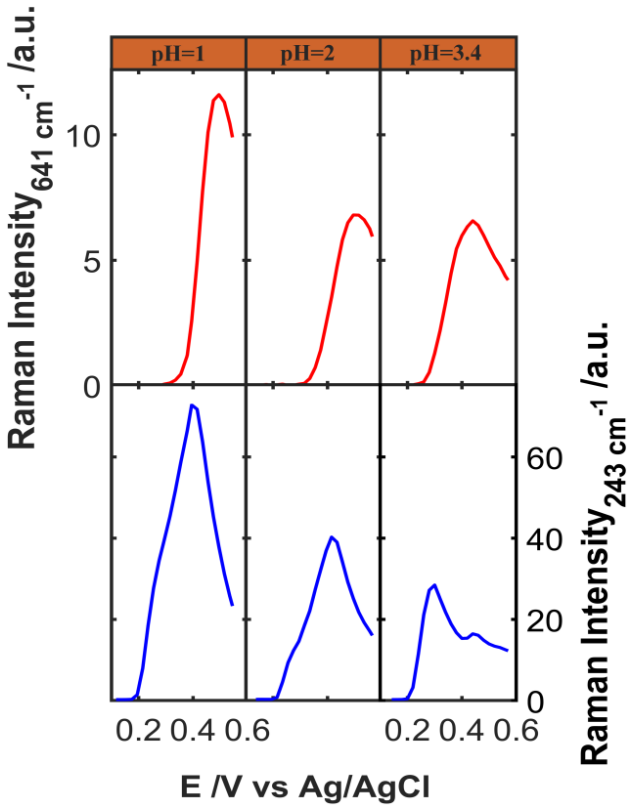

ACCEPTED MANUSCRIPT

ACCEPTED MANUSCRIPT

Figure 5.

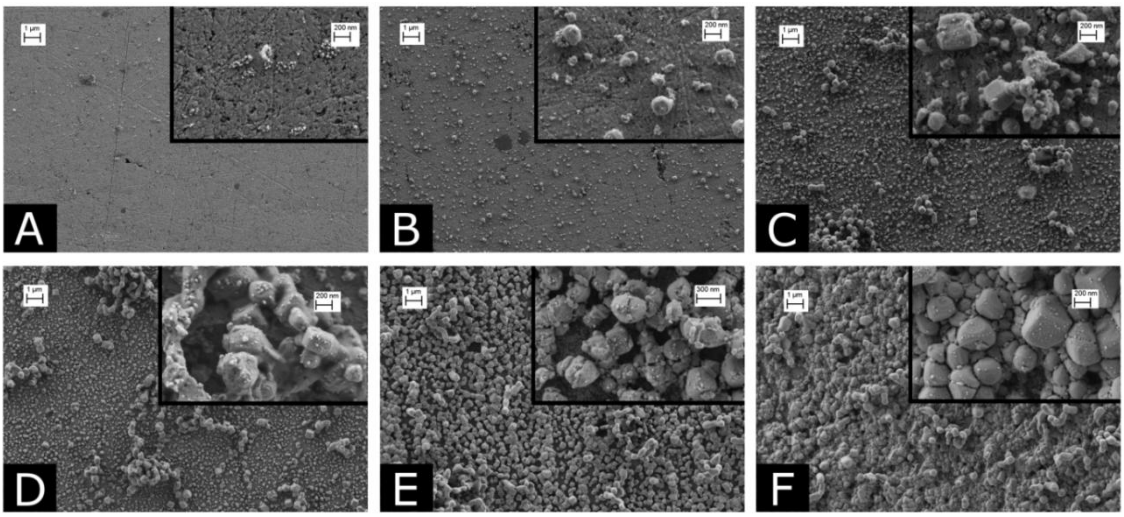

ACCEPTED MANUSCRIPT

ACCEPTED MANUSCRIPT

Figure 6.

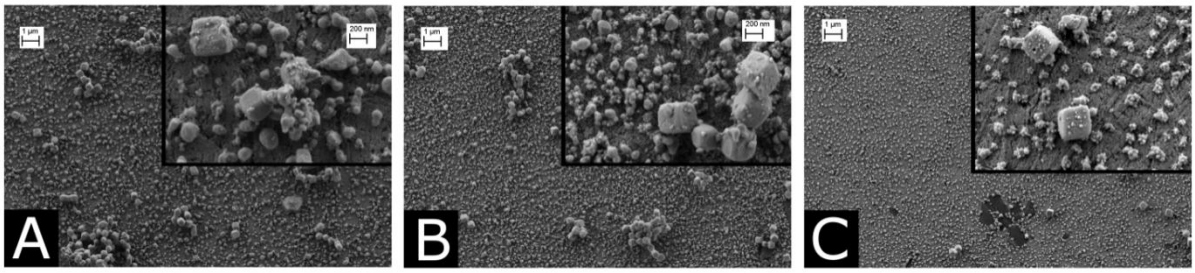

ACCEPTED MANUSCRIPT

ACCEPTED MANUSCRIPT

Tables

Table 1. Evolution of the onset potential and the Raman intensity at the maximum for the voltaRamangram at 641 cm^{-1} with the Cl^- concentration for UA $2 \cdot 10^{-4}$ M + $HClO_4$ 0.1 M + KCl X M. Results were taken from the experiments shown in Figure 3. The minimum values for the onset potential and the maximum values for the Raman intensity are listed in bold.

[Cl⁻] / mM	**E_{onset} / V vs Ag/AgCl**	**Raman I_{max} / a.u.**
0.05	0.387	553
0.5	0.350	848
1	0.329	1851
5	**0.295**	**11600**
10	**0.255**	**12400**
50	0.331	4588
100	0.395	1078

Table 2. Evolution of the onset potential and the Raman intensity at the maximum for the voltaRamangram at 641 cm^{-1} at different pH values for UA $2 \cdot 10^{-4}$ M + $HClO_4$ X M + $KClO_4$ (0.1-X) M + KCl $5 \cdot 10^{-3}$ M. Results were taken from the experiments shown in Figure 4.

pH	**E_{onset} / V vs Ag/AgCl**	**Raman I_{max} / a.u.**
1	0.295	11600
2	0.275	6802
3.4	0.220	6574

ACCEPTED MANUSCRIPT

Graphical abstract